Available online at www.sciencedirect.com
SCIENCE DIRECT®

Journal of the European Ceramic Society 24 (2004) 2631–2639

www.elsevier.com/locate/jeurceramsoc

Phase interaction and oxygen transport in $La_{0.8}Sr_{0.2}Fe_{0.8}Co_{0.2}O_3$–$(La_{0.9}Sr_{0.1})_{0.98}Ga_{0.8}Mg_{0.2}O_3$ composites

A.L. Shaula[a], V.V. Kharton[a,b,*], F.M.B. Marques[a]

[a]*Department of Ceramics and Glass Engineering, CICECO, University of Aveiro, 3810-193 Aveiro, Portugal*
[b]*Institute of Physicochemical Problems, Belarus State University, 14 Leningradskaya Str., 220050 Minsk, Belarus*

Received 16 July 2003; received in revised form 19 September 2003; accepted 27 September 2003

Abstract

Composite ceramics made of two perovskite-type compounds, $(La_{0.9}Sr_{0.1})_{0.98}Ga_{0.8}Mg_{0.2}O_{3-\delta}$ (LSGM) and $La_{0.8}Sr_{0.2}Fe_{0.8}Co_{0.2}O_{3-\delta}$ (LSFC) mixed in the ratio 60:40 wt.%, possess relatively high oxygen permeability limited by both bulk ionic conduction and surface exchange at 700−950 °C. Sintering at elevated temperatures (1320–1410 °C) necessary to obtain dense materials leads to fast interdiffusion of the components, forming almost single perovskite phase ceramics with local inhomogeneities. This phase interaction decreases the oxygen ionic transport in the composites, where the level of ionic conductivity is intermediate between those of LSGM and LSFC. The scanning electron microscopy (SEM) suggests a presence of Ga-enriched domains, probably having a high ionic conductivity. The size and concentration of these domains can be increased by decreasing sintering temperature or using preliminary coarsened LSGM powders. The maximum oxygen permeability is thus observed for the composite prepared under minimum sintering conditions sufficient to obtain gas-tight ceramics, including the use of LSGM, preliminary passivated at 1150 °C, and sintered at 1320 °C. The activation energy values for total conductivity, which is predominantly p-type electronic and slightly decreases due to component interaction, vary in the narrow range from 24.0 to 26.2 kJ/mol at 25–575 °C. The average thermal expansion coefficients (TECs) of LSGM-LSFC composites, calculated from dilatometric data in air, are (12.4–13.5)×10^{-6} K^{-1} at 100–650 °C and (17.8–19.8)×10^{-6} K^{-1} at 650–1000 °C.

Keywords: Composites; Ionic conductivity; (La,Sr)(Fe,Co)O_3; (La,Sr)(Ga,Mg)O_3; Membranes; Mixed conductor; Perovskites

1. Introduction

Ceramic materials with mixed oxygen ionic and electronic conductivity are of great interest for high-temperature electrochemical devices, such as solid oxide fuel cells (SOFCs), electrocatalytic reactors, oxygen separation membranes and sensors.[1,2] However, for practical applications mixed-conducting ceramics should satisfy to numerous criteria, including appropriate transport properties, thermodynamic and dimensional stability under operation conditions, and moderate thermal expansion coefficients compatible with other components of electrochemical cells.[2,3] In particular, perovskite-like phases (A,Ln)$MO_{3-\delta}$ (A = Ca, Sr, Ba; M = Fe, Co; Ln is rare-earth element) show attractive oxygen permeation fluxes, but often are thermodynamically unstable under large oxygen chemical potential gradients; ordering in the oxygen sublattice of such materials and high reactivity with gaseous species, such as CO_2, leads to a degradation of oxygen transport properties with time.[4–6]

One interesting group of mixed-conductive ceramic membranes relates to dual-phase composites, where a solid electrolyte phase is mixed with a material showing high electronic transport.[2,7] In this case, optimisation of transport and physicochemical properties may include variations in the compositions of both phases and in their ratio. At the same time, the resultant properties may be strongly dependent of the interaction between the components. For example, the ionic transport in $Ce_{0.8}Gd_{0.2}O_{2-\delta}$ (CGO)– $La_{0.7}Sr_{0.3}MnO_{3-\delta}$ (LSM) membranes was found to decrease due to cation interdiffusion between phases.[8,9] In addition, CGO-LSM composites comprising significant volume fractions of

* Corresponding author. Tel.: +351-234-370263; fax: +351-234-425300.
E-mail address: kharton@cv.ua.pt (V.V. Kharton).

0955-2219/$ - see front matter © 2003 Elsevier Ltd. All rights reserved.
doi:10.1016/j.jeurceramsoc.2003.09.021

CGO may be unstable under large oxygen pressure gradients due to significant volume changes of ceria on reducing. A better performance of dual-phase membranes could be expected using a more stable solid-electrolyte phase instead of CGO, and also substituting LSM with a mixed conductor, which may contribute to ionic transport. Therefore, in this work composite materials consisting of $(La_{0.9}Sr_{0.1})_{0.98}Ga_{0.8}Mg_{0.2}O_{3-\delta}$ (LSGM) as an ionic conductor and mixed-conducting $La_{0.8}Sr_{0.2}Fe_{0.8}Co_{0.2}O_{3-\delta}$ (LSFC) were examined. The perovskite-type solid electrolytes based on lanthanum gallate are well known for their high oxygen ionic conduction and stability in a wide range of oxygen partial pressures; the advantages of $La(Sr)Fe(Co)O_{3-\delta}$ perovskites include a significant ionic contribution to the total conductivity, predominantly *p*-type electronic in oxidising conditions, and moderate thermal expansion coefficients (TECs).[2,4,6]

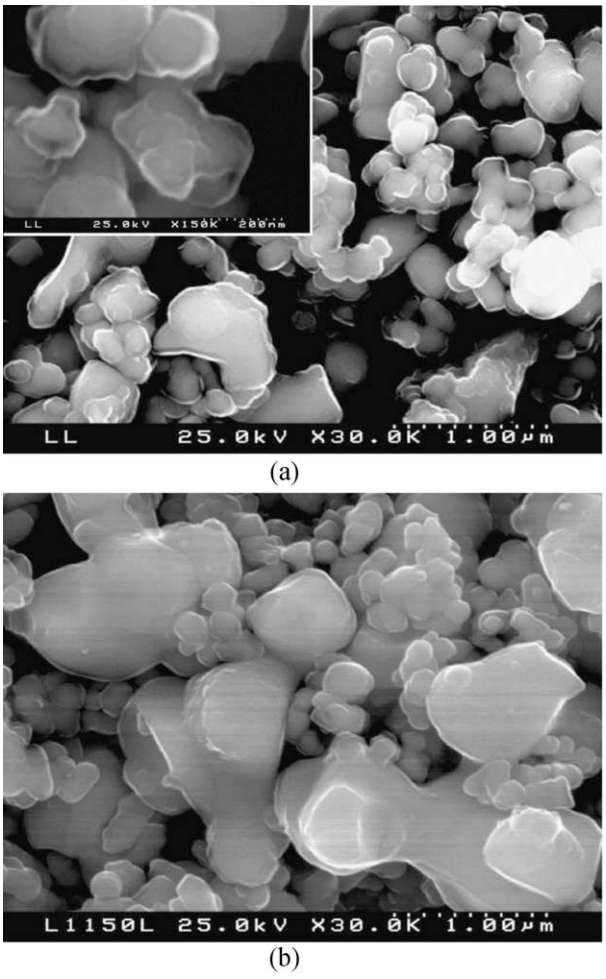

Fig. 1. SEM micrographs of LSGM–LSFC powders obtained by Method 1 (A) and Method 2 (B).

2. Experimental

Dense ceramic samples of LSGM-LSFC composites were produced using commercial powders of $(La_{0.9}Sr_{0.1})_{0.98}Ga_{0.8}Mg_{0.2}O_{3-\delta}$ and $La_{0.8}Sr_{0.2}Fe_{0.8}Co_{0.2}O_{3-\delta}$ (Praxair Speciality Chemicals, Seattle). Taking into account data on CGO–LSM ceramics[8] showing that the fraction of the ion-conducting phase may be critical for the oxygen permeation level, the LSGM/LSFC ratio was selected as 60:40 wt.%. To study the influence of the interaction between initial phases on the final product properties, the LSGM–LSFC mixtures were prepared by different procedures. One series of composite ceramics, marked as LL, was fabricated via ball-milling of the commercial powders for 6 h in ethanol medium (Method 1). For another series (LLc), the LSGM powder was coarsened by annealing at 1150 °C during 4 h and then mixed with LSFC powder in an agate mortar (Method 2). Fig. 1 compares SEM micrographs of LSGM-LSFC powders obtained by these two techniques. Both mixtures were uniaxially pressed (250–300 MPa) into disks and sintered in atmospheric air with heating/cooling rates of 10 °C/min. The sintering conditions and corresponding abbreviations are listed in Table 1. As an example, LLc1320 relates to composite ceramics prepared by Method 2 and sintered at 1320 °C. After sintering, the samples were annealed at 1000 °C in air for 4 h and then slowly furnace-cooled in order to achieve oxygen nonstoichiometry as close as possible to the equilibrium at low temperatures.

Table 1
Abbreviations and processing conditions

Composition	Abbreviation	Pre-annealling of LSGM		Sintering		Gas-tightness
		T, °C	Time, h	T, °C	Time, h	
$(La_{0.9}Sr_{0.1})_{0.98}Ga_{0.8}Mg_{0.2}O_{3-\delta}$	LSGM	–	–	1400	4	+
$La_{0.8}Sr_{0.2}Fe_{0.8}Co_{0.2}O_{3-\delta}$	LSFC	–	–	1400	4	+
Composite 60% (wt.) LSGM/40% (wt.) LSFC	LL1240	–	–	1240	1	–
	LL1320	–	–	1320	1	+
	LLc1320	1150	4	1320	1	+
	LL1410	–	–	1410	4	+
	LLc1410	1150	4	1410	4	+

Table 2
Properties of LSGM, LSFC and composite ceramics

Composition	Space group	Unit cell parameters			ρ_{exp}, g/cm^3	ρ_{exp}/ρ_{theor},%	Thermal expansion coefficients		Activation energy for total conductivity		
		a, nm	b, nm	c, nm			T, °C	$\bar{\alpha}\times10^6$, K^{-1}	T, °C	E_a, kJ/mol	ln(A_0), S*K/cm
LSFC	R$\bar{3}$c	0.5521	–	1.3376	6.14	94.0	100–800	12.9±0.2	150–620	12.3±0.5	13.5±0.1
LSGM	I2/a	0.7829	0.5546	0.5528	6.24	95.2	100–1000	11.1±0.1	370–950	96±7	15±1
LL1320	R$\bar{3}$c	0.5525	–	1.3394	6.25	94.6	100–650	12.81±0.01	25–575	26.2±0.5	12.1±0.1
							650–1000	18.96±0.01			
LLc1320	R$\bar{3}$c	0.5525	–	1.3385	6.18	93.5	100–650	13.48±0.01	25–575	24.0±0.3	12.2±0.1
							650–1000	17.79±0.01			
LL1410	R$\bar{3}$c	0.5526	–	1.3392	6.22	94.2	100–650	12.36±0.01	25–575	25.1±0.5	11.9±0.1
							650–1000	19.75±0.02			
LLc1410	R$\bar{3}$c	0.5527	–	1.3385	6.33	95.9	100–650	12.63±0.01	25–575	24.9±0.2	12.1±0.1
							650–1000	18.98±0.01			

The prepared LSGM–LSFC composites were characterised by X-ray diffraction (XRD), dilatometry, scanning electron microscopy combined with energy dispersive spectroscopy (SEM/EDS), and by measurements of total conductivity by 4-probe DC technique. The XRD patterns were collected at room temperature using a Rigaku D/MAX-B diffractometer (CuK_α, $2\Theta = 20$–$80°$, step 0.02°, 1 s/step). Structural parameters were refined from XRD data using the Fullprof program.[10] The density of ceramic materials was 94–96% of their theoretical density calculated from XRD results (Table 2). Thermal expansion and shrinkage were measured using an alumina Linseis L70 dilatometer with a constant heating rate of 5 °C/min, in air. SEM studies were performed using a Hitachi S-4100 microscope equipped with a Rontec UHV Detection system for the EDS analysis. The oxygen ionic transport properties were evaluated using the measurements of steady-state oxygen permeation fluxes, as described elsewhere.[11] Only gas-tight samples were used for the permeation studies. All data on oxygen permeability presented in this work correspond to the membrane feed-side oxygen partial pressure (p_2) maintained at 21 kPa (atmospheric air); the permeate-side oxygen partial pressure (p_1) varied in range 0.2–20 kPa. Detailed description of the equipment and techniques, used for ceramics characterisation and oxygen permeation measurements, was published earlier.[11–15]

3. Results and discussion

3.1. Phase composition and microstructure

XRD analysis of all LSGM–LSFC composite ceramics indicated an apparent formation of one single perovskite-type phase with a rhombohedral distortion, typical for LSFC. The unit cell parameters (a and c) are given in Table 2. Fig. 2 compares XRD patterns of LSGM, LSFC and LLc1320 composite, where the component interaction was minimum compared to other gas-tight ceramics. The solid-state interaction between these phases occurs considerably faster than that in LSM–CGO composites where the components have different lattices. In the latter case, sintering at 1500–1600 °C resulted in moderate reaction, mainly associated with diffusion of A-site cations of LSM into ceria.[8,9]

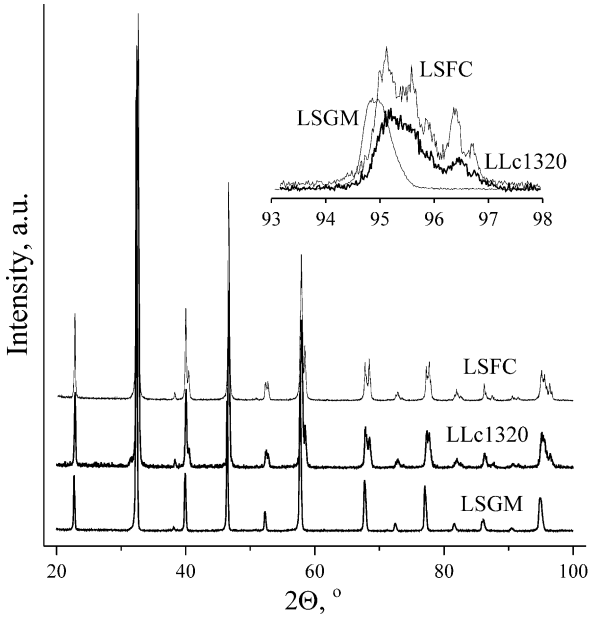

Fig. 2. XRD patterns of LSGM, LSFC and composite LLc1320.

At the same time, for complete reaction the result would be a single perovskite phase having the total composition $La_{0.849}Sr_{0.139}Ga_{0.476}Fe_{0.324}Mg_{0.119}Co_{0.081}O_{3-\delta}$. Fig. 3 compares the theoretical unit cell volume of this phase, estimated assuming a linear volume dependence on the

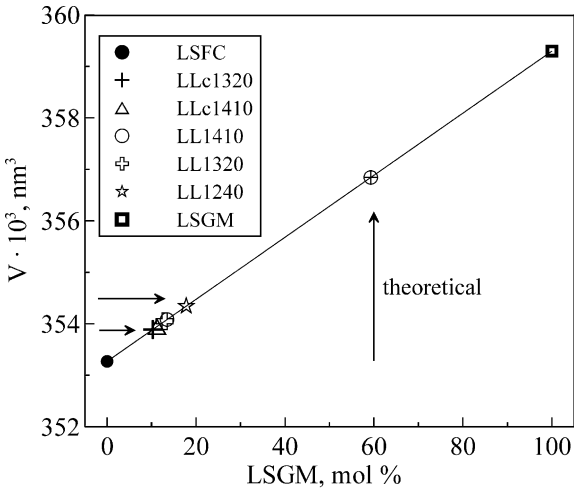

Fig. 3. Unit cell volume of LSGM, LSFC and LSGM–LSFC perovskite phases. Volume of monoclinic unit cell of LSGM is normalised to six formula units, as for rhombohedrally-distorted perovskite in hexagonal settings. The vertical arrow shows the theoretical volume estimated from the molar fractions of the components, assuming linear dependence of the volume on composition.

composition (Vegard's rule), with the experimental values calculated from XRD data. Although a simple Vegard-type relation cannot be observed in this case as the lattice of LSGM is monoclinically-distorted (space group I2/a),[16] data in Fig. 3 unambiguously shows that the average lattice parameters in LSGM–LSFC composites are far from the level expected in the case of complete interdiffusion. In fact, the apparent unit cell volume of all composite materials is close to that of the LSFC phase. This suggests that the interaction in the course of sintering occurs primarily via diffusion of iron and cobalt cations into LSGM grains. If the mobility of these ions is higher than that of Ga^{3+}, one might expect an existence of Ga-enriched domains, whereas the remaining volume of composite materials should be Fe-enriched with respect to the equilibrium composition.

The microstructures of polished LSGM-LSFC samples are compared in Fig. 4. SEM studies confirmed a relatively good quality of the ceramic materials, in particular low porosity. The sintering temperature and preliminary annealing of LSGM powder have no sig-

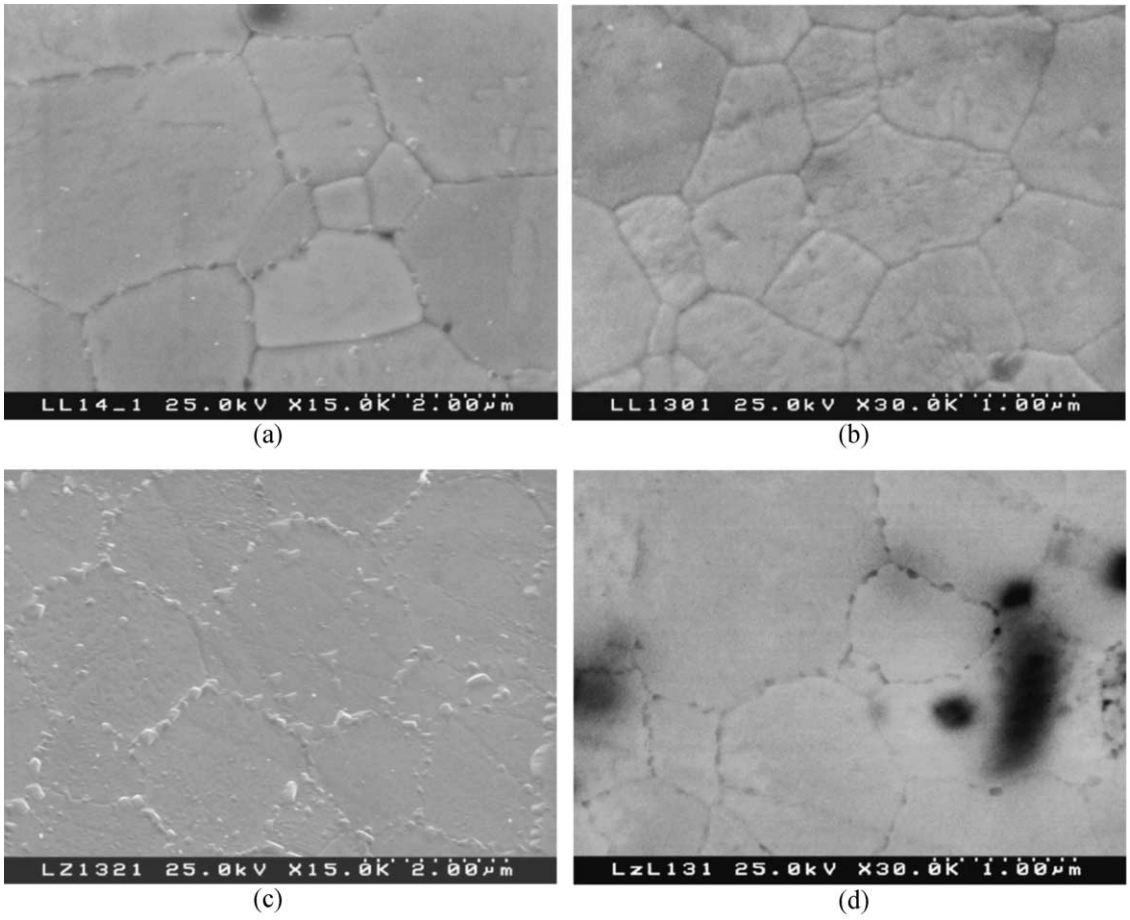

Fig. 4. SEM micrographs of composite ceramics: LL1410 (A), LLc1410 (B), LL1320 (C) and LLc1320 (D). The micrograph D was obtained in back-scattering mode.

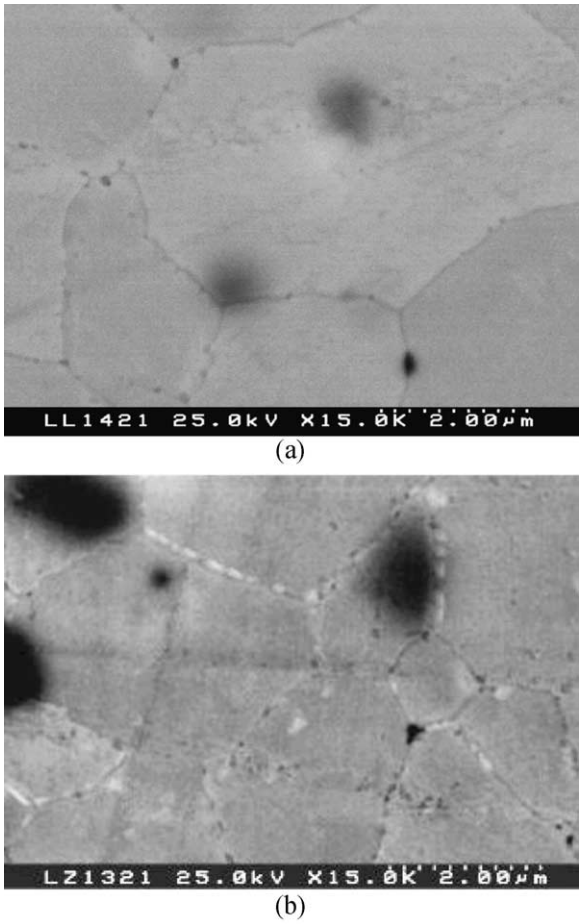

Fig. 5. Back-scattered SEM micrographs of LL1410 (A) and LLc1410 (B) ceramics.

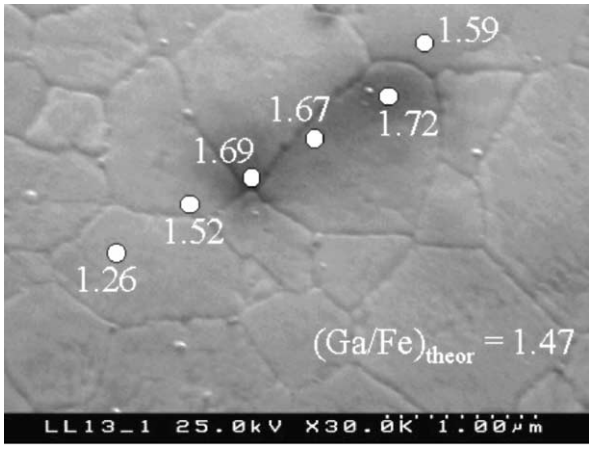

Fig. 6. SEM micrograph of LL1320 ceramics. The atomic Ga/Fe ratios in several points were evaluated by EDS analysis.

nificant influence on the average grain size, varying for all LSGM–LSFC composites in the narrow range 1–3 μm. The use of SEM back-scattering mode showed local inhomogeneities visible as dark regions of ceramic grains (Fig. 4D). The size and content of these domains

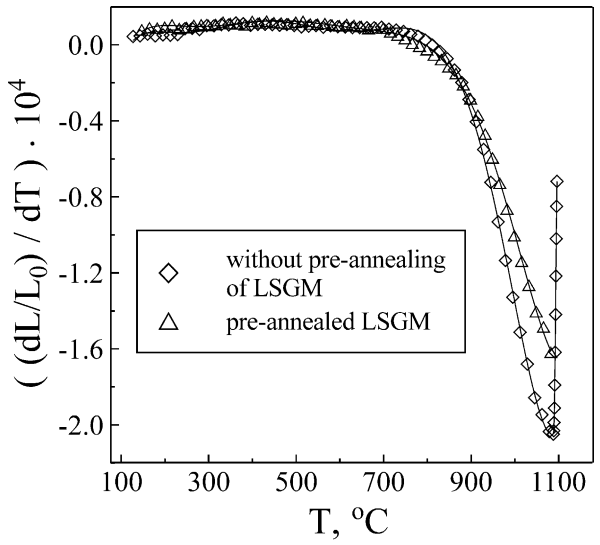

Fig. 7. Differential shrinkage curves for LL and LLc green compacts.

increased when using coarsened LSGM and when the sintering temperature decreases. This is illustrated in Fig. 5, comparing back-scatter SEM micrographs of two composites, LL1410 and LLc1410, both sintered at the 1410 °C. The EDS analysis indicated that the chemical composition in these domains is certainly different from the average composition. As an example, Fig. 6 presents the distribution of the Ga/Fe concentration ratio in several positions; the dark domain is enriched with gallium, while the neighbouring grains are Ga-depleted. Hence, as expected, the solid-state reaction of LSGM and LSFC phases in the course of sintering is not complete. The prepared composites are not homogeneous; the level of inhomogeneity may increase by decreasing sintering temperature and preliminary coarsening of LSGM. One should note, however, that for the LL1320 and LLc1320 series the sintering temperature and time were close to the minimum necessary to obtain gas-tight ceramics. Attempts to obtain dense materials with low level of interaction between LSGM and LSFC, particularly by sintering at 1240 °C for 1 h and by coarsening both components, failed.

3.2. Dilatometric studies

As described before, different powder preparation procedures were used for the LL and LLc series (Methods 1 and 2, respectively). After sintering of ball-milled powders resulted in almost complete solid-state reaction between the phases, the latter procedure was employed in order to decrease LSGM reactivity. However, despite of coarsening and shorter sintering periods, the phase interaction detected by XRD and SEM/EDS was still significant. Dilatometric tests of green compacts (Fig. 7) confirmed that the active shrinkage processes, probably associated with cation interdiffusion, start at

approximately 850–1000 °C. Although the use of coarsened LSGM powder (Method 2) results in lower shrinkage, it has no essential effect on the starting sintering temperature. This suggests, in particular, that interaction between the LSGM electrolyte and perovskite cathodes based on $LaMO_3$ (M = Fe, Co), used for intermediate-temperature SOFCs,[17,18] may occur at the cell fabrication temperatures, 1000–1150 °C.

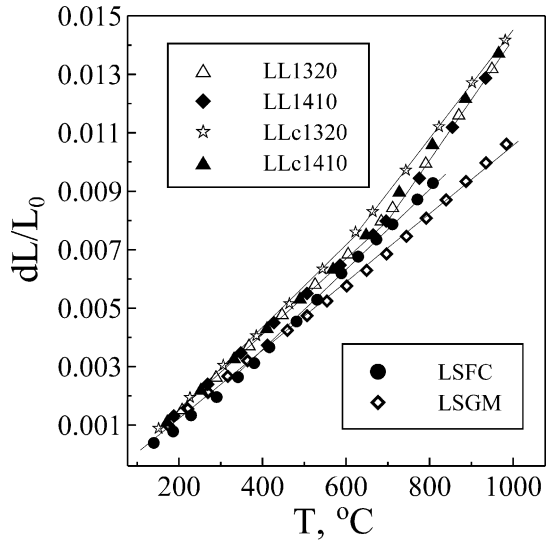

Fig. 8. Thermal expansion of LSGM–LSFC composite ceramics in air.

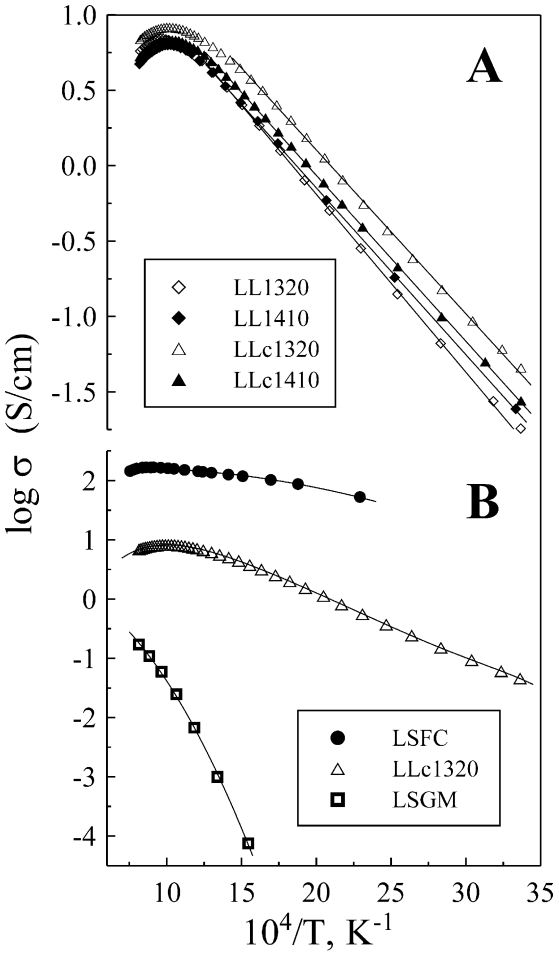

Fig. 9. Temperature dependence of total conductivity in air.

The dilatometric curves of dense LSGM–LSFC materials are non-linear, with a break at 600–700 °C (Fig. 8). At 100–650 °C, the average thermal expansion coefficients (TECs) vary in the range $(12.4–13.5)\times10^{-6}$ K^{-1}, which is quite similar to the TEC of single-phase LSFC ceramics (Table 2). Further heating leads to increasing TEC values up to $(17.8–19.8)\times10^{-6}$ K^{-1}. Such a behaviour is typical for Fe-containing ceramic materials and results from oxygen losses on heating, providing an additional chemical contribution to the lattice thermal expansion.[19,20] It should be mentioned that the TEC values of LSGM–LSFC ceramics are considerably higher than that of the $LaGaO_3$-based solid electrolyte, although the starting content of LSGM in the composites is 60 wt.% (approximately 59 mol%). This enhances the role of inhomogeneous cation distribution on the overall materials performance. Most probably, the high TECs of these composite ceramics are associated with the Fe-enriched volume, while the Ga-rich domains possess lower expansion. As a result, lower sintered temperatures and use of coarsened LSGM powder, which provides larger Ga-enriched domains (Fig. 5), lead to decreasing TECs in the high-temperature range (Table 2).

3.3. Total conductivity

Fig. 9 presents the temperature dependencies of total conductivity (σ) of LSGM–LSFC ceramics in air. Data on oxygen permeability, discussed below, suggests that the oxygen ion transference numbers are lower than 0.03; the total conductivity is predominantly *p*-type electronic. As expected, the general trends in behaviour of LSGM–LSFC ceramics are similar to LSFC, whilst the values of σ are 10–30 times lower (Fig. 9B). At 25–600 °C, the conductivity of composites follows an Arrhenius dependence; further heating leads to oxygen losses, decreasing electron-hole concentration and, thus, decreasing σ. These tendencies are in excellent agreement with literature on $LaFeO_3$- and $SrFeO_3$-based systems,[3,19–21] where the dominant *p*-type electronic transport occurs via small-polaron mechanisms and increasing oxygen nonstoichiometry on heating results in apparent pseudometallic behaviour.

The values of activation energy (E_a) for the total conductivity in low-temperature range, calculated by the standard Arrhenius equation

$$\sigma = \frac{A_0}{T}\exp\left[-\frac{E_a}{RT}\right] \quad (1)$$

where A_0 is the pre-exponential factor, are listed in Table 2. For LSGM–LSFC ceramics, the activation

energy varies from 24.0 to 26.2 kJ/mol, which is higher than the corresponding value for LSFC (12.3 kJ/mol), but four times lower than the activation energy for the ionically-conductive LSGM (96 kJ/mol).

Increasing interaction level between LSGM and LSFC phases results in a moderate decrease of the total conductivity. With respect to other composite materials, the highest total conductivity values were observed for LLc1320, where the inhomogeneity of ceramics is maximum. It is well known for $LaGaO_3$–$LaMO_3$ (M = Fe, Co, Ni) systems[12,13,15] that incorporation of insulating Ga^{3+} cations, having stable oxidation state, blocks electronic transport in transition metal-containing perovskites. Therefore, as for thermal expansion, the total conductivity of LSGM–LSFC composites is determined by iron-enriched fraction.

3.4. Oxygen ionic transport

The oxygen permeation fluxes (j) through dense LSGM–LSFC membranes are plotted in Fig. 10A as a function of the oxygen partial pressure gradient and membrane thickness (d). The corresponding values of specific oxygen permeability, $J(O_2)$, shown in Fig. 10B were calculated as[4,8,11]

$$j = \frac{J(O_2)}{d} \cdot \ln\left(\frac{p_2}{p_1}\right) \quad (2)$$

The quantity $J(O_2)$ is suitable to identify a limiting effect of surface exchange rate on the oxygen permeation.[4] This quantity is, by definition, proportional to $j \times d$, and should thus be independent of thickness in the case when surface limitations are negligible. In this situation, $J(O_2)$ is proportional to the so-called ambipolar conductivity (σ_{amb}), averaged for a given oxygen partial pressure range:

$$\sigma_{amb} = \frac{16F^2 \times J(O_2)}{RT} = \frac{\sigma_O\ \sigma_e}{\sigma_O + \sigma_e} = t_O(1 - t_O) \times \sigma \quad (3)$$

where t_o is the oxygen ionic transference number, σ, σ_o and σ_e represent the total, oxygen ionic and electronic conductivities, respectively. When oxygen exchange limitations are considerable, $J(O_2)$ should increase with increasing membrane thickness, for a given oxygen chemical potential gradient, due to a decreasing role of the surface exchange.

The latter situation is observed for LSGM-LSFC ceramics (Fig. 10). At 900–950°C, the values of $J(O_2)$ increase and the oxygen fluxes decrease with increasing membrane thickness. This unambiguously indicates that the overall oxygen transport is affected by bulk ambipolar conductivity and surface exchange rate. When the temperature decreases, the role of exchange kinetics as permeation-limiting factor increases; the oxygen fluxes tend to be thickness-independent. A similar behaviour, which is typical for single-phase $La(Sr)Ga(M,Mg)O_{3-\delta}$ (M = Fe, Co, Ni) heavily doped with acceptor-type cations,[22,23] was observed for all LSGM-LSFC composites studied in this work.

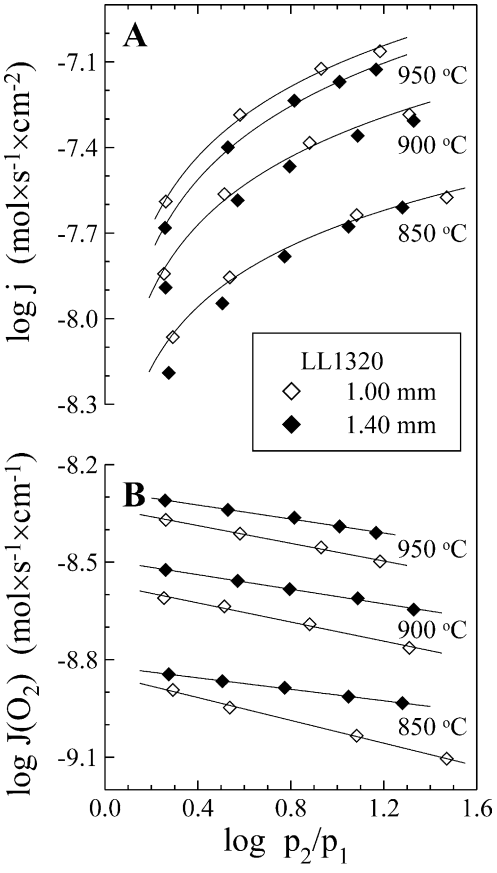

Fig. 10. Dependence of the oxygen permeation fluxes (A) and specific oxygen permeability (B) of LL1320 membranes on the oxygen partial pressure gradient. Feed-side oxygen pressure (p_2) is 21 kPa.

Fig. 11 compares the oxygen permeation fluxes through LSGM–LSFC membranes under a fixed oxygen pressure gradient. As for the total conductivity, a maximum oxygen permeability is observed for LLc1320 ceramics, where the interaction degree between LSGM and LSFC phases is minimum compared to other composite materials. The permeability of LLc1320 is quite high; for example, an oxygen flux of 1.1×10^{-7} mol×cm^{-2}×s^{-1} was measured through a 1.0 mm thick membrane placed under a $p(O_2)$ gradient of 21/2.1 kPa at 950−C. This level of oxygen permeability is similar to that of single-phase materials having similar cationic composition, such as $La_{0.8}Sr_{0.2}Ga_{0.6}Mg_{0.2}M_{0.2}O_{3-\delta}$ (M = Fe, Co)[22] or $LaGa_{0.65}Ni_{0.2}Mg_{0.15}O_{3-\delta}$[23] (Fig. 11B).

The estimates of oxygen ionic conductivity which can be obtained using Eq. (3), are lower than the true values due to significant surface exchange limitations to oxygen permeation fluxes (Fig. 10). Nonetheless, such an estimation might be of interest in order to reveal factors

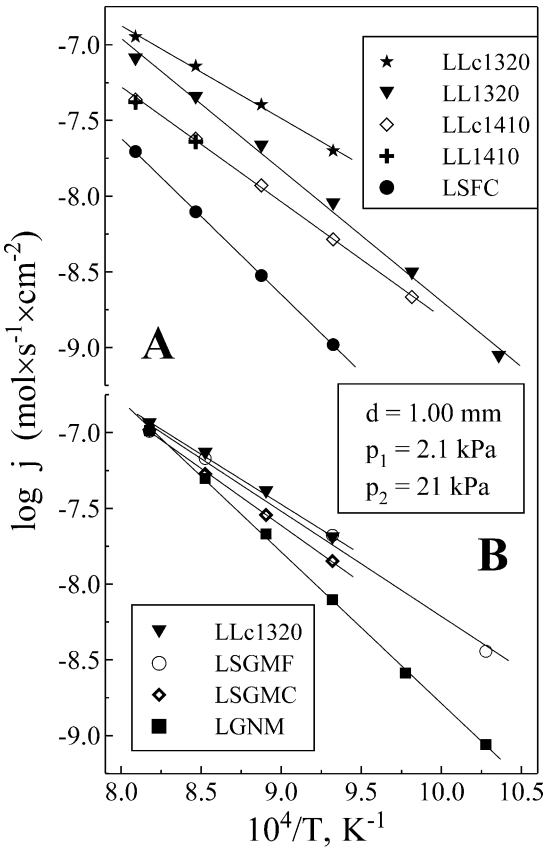

Fig. 11. Temperature dependence of the oxygen permeation fluxes through LSGM-LSFC composite ceramics at fixed oxygen partial pressure gradient. Membrane thickness is 1.00 mm. Data on single-phase $La_{0.8}Sr_{0.2}Ga_{0.6}Mg_{0.2}Co_{0.2}O_{3-\delta}$ (LSGMC),[22] $La_{0.8}Sr_{0.2}Ga_{0.6}Mg_{0.2}Fe_{0.2}O_{3-\delta}$ (LSGMF)[22] and $LaGa_{0.65}Ni_{0.2}Mg_{0.15}O_{3-\delta}$ (LGNM)[23] are shown for comparison.

affecting the level of bulk ambipolar conduction. Fig. 12 presents the temperature dependencies of apparent ionic conductivity in LSGM–LSFC composites, calculated from the oxygen permeation fluxes through 1.0 mm thick membranes. Data on LSGM and LSFC, shown for comparison, correspond to the true ionic conductivity of these compositions. In the latter case, the ionic conductivity was directly measured by impedance spectroscopy as the oxygen ion transference numbers measured by the faradaic efficiency technique are higher than 0.99. For LSFC membranes, no surface effect on the oxygen permeation fluxes was observed. The apparent ionic conductivity of LLc1320 ceramics, exhibiting maximum oxygen transport with respect to other LSGM–LSFC composites, is 4–50 times lower than the conductivity of LSGM. The level of ionic conduction in LSGM–LSFC ceramics is, therefore, presumably the result of the contribution of Ga-rich domains and decreases due to phase interaction, with dissolution of gallium cations in the lattice.

In summary, the cation interdiffusion between LSGM and LSFC perovskite phases has a deteriorating influence on the transport properties. In the case of electronic

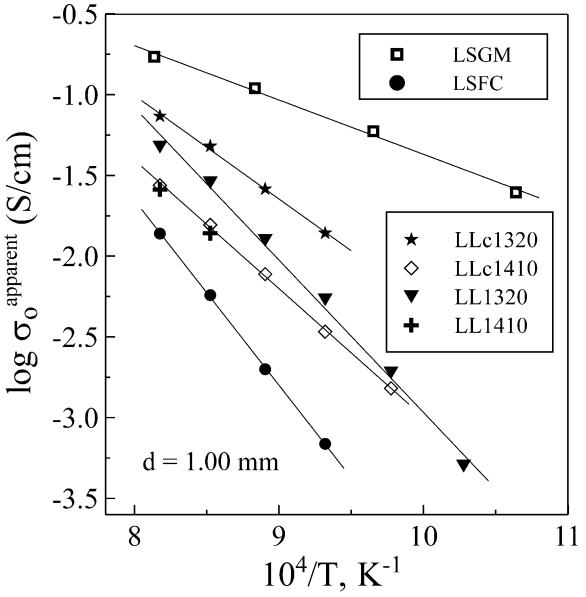

Fig. 12. Comparison of ionic conductivity in LSGM, LSFC and LSGM–LSFC ceramics (see text).

conduction, this effect is rather small (Fig. 9); the influence of phase interaction on the oxygen ionic transport may be critical (Fig. 12). The processing conditions of solid oxide fuel cells, made of $LaGaO_3$-based solid electrolytes and perovskite cathodes based on $LaMO_3$ (M = Fe, Co),[17,18] should hence be optimised in order to prevent interdiffusion between electrolyte and electrode materials. For oxygen separation membranes, sintering of dual-phase composite ceramics consisting of LSGM and LSFC is inappropriate as the resultant properties are strongly dependent on phase interaction. Even for optimised membrane microstructures with maximum oxygen transport, this may lead to degradation processes in the course of long-term operation at elevated temperatures. These problems can be solved using vapour deposition techniques for the preparation of film membranes operating at temperatures below 800 °C.

4. Conclusions

The perovskite-type solid electrolyte, $(La_{0.9}Sr_{0.1})_{0.98}Ga_{0.8}Mg_{0.2}O_{3-\delta}$ (LSGM), and mixed-conducting $La_{0.8}Sr_{0.2}Fe_{0.8}Co_{0.2}O_{3-\delta}$ (LSFC) phases possess similar thermal expansion coefficients (TECs) and were thus combined in composites with weight LSGM/LSFC ratio of 60:40. The fast cation interdiffusion between these phases was found to decrease both ionic and electronic conductivities and to increase thermal expansion. Sintering of the composites at 1320–1410 °C, which is necessary to obtain dense ceramics, leads to formation of almost single-phase materials with local inhomogeneities, such as Ga-enriched domains. Since the ionic conductivity level of LSGM–LSFC composites varies

between those of parent compounds, local enrichment with gallium is supposed to increase the local ionic transport. Indeed, the maximum oxygen permeation was observed for composite membranes prepared under conditions providing minimum interaction, but sufficient to obtain gas-tight ceramics. These conditions include the use of LSGM powder, preliminary passivated at 1150 °C, and sintered at 1320 °C for 1 h. The total conductivity of LSGM–LSFC materials is predominantly *p*-type electronic, with activation energy of 24.0–26.2 kJ/mol at 25–575 °C. The oxygen permeation fluxes through LSGM-LSFC membranes at 700–950 °C are limited by both bulk ionic conduction and surface exchange kinetics.

Acknowledgements

This work was supported by the FCT, Portugal (POCTI program and project BD/6595/2001), by the NATO Science for Peace program (project 978002), and by the INTAS (project 00276).

References

1. Balachandran, U., Dusek, J. T., Sweeney, S. M., Poeppel, R. B., Mieville, R. L., Maiya, P. S., Kleefisch, M. S., Pei, S., Kobylinski, T. P., Udovich, C. A. and Bose, A. C., Methane to syngas via ceramic membranes. *Am. Ceram. Soc. Bull.*, 1995, **74**, 71–75.
2. Bouwmeester, H. J. M. and Burggraaf, A. J., Dense ceramic membranes for oxygen separation. In *Fundamentals of Inorganic Membrane Science and Technology*, ed. A. J. Burggraaf and L. Cot. Elsevier, Amsterdam, 1996, pp. 435–528.
3. Anderson, H. U., Review of p-type doped perovskite materials for SOFC and other applications. *Solid State Ionics*, 1992, **52**, 33–41.
4. Kharton, V. V., Yaremchenko, A. A., Kovalevsky, A. V., Viskup, A. P., Naumovich, E. N. and Kerko, P. F., Perovskite-type oxides for high-temperature oxygen separation membranes. *J. Membr. Sci.*, 1999, **163**, 307–317.
5. Kruidhof, H., Bouwmeester, H. J. M., van Doorn, R. H. E. and Burggraaf, A. J., Influence of order-disorder transitions on oxygen permeability through selected nonstoichiometric perovskite-type oxides. *Solid State Ionics*, 1993, **63-65**, 816–822.
6. Teraoka, Y., Zhang, H. M., Furukawa, S. and Yamazoe, N., Oxygen permeation through perovskite-type oxides. *Chem. Lett.*, 1985, **11**, 1743–1746.
7. Shen, Y. S., Liu, M., Taylor, D., Balagopal, S., Joshi, A. and Krist, K., Mixed ionic-electronic conductors based on Bi-Y-O-Ag metal-ceramic system. In *Proc. of 2nd Int. Symp. on Ionic and Mixed Conducting Ceramics*, ed. T. A. Ramanarayanan, W. L. Worrell and H. L. Tuller. The Electrochemical Society, Pennington, NJ, 1994, pp. 574–595 94-12.
8. Kharton, V. V., Kovalevsky, A. V., Viskup, A. P., Figueiredo, F. M., Yaremchenko, A. A., Naumovich, E. N. and Marques, F. M. B., Oxygen permeability $Ce_{0.8}Gd_{0.2}O_{2-\delta}$–$La_{0.7}Sr_{0.3}MnO_{3-\delta}$ composite membranes. *J. Electrochem. Soc.*, 2000, **147**, 2814–2821.
9. Kharton, V. V., Kovalevsky, A. V., Viskup, A. P., Figueiredo, F. M., Yaremchenko, A. A., Naumovich, E. N. and Marques, F. M. B., Oxygen permeability and faradaic efficiency of $Ce_{0.8}Gd_{0.2}O_{2-\delta}$–$La_{0.7}Sr_{0.3}MnO_{3-\delta}$ composites. *J. Eur. Ceram. Soc.*, 2001, **21**, 1763–1767.
10. Rodriguez-Carvajal, J., Recent advances in magnetic-structure determination by neutron powder diffraction. *Physica B*, 1993, **192**, 55–69.
11. Kharton, V. V., Tikhonovich, V. N., Shuangbao, L., Naumovich, E. N., Kovalevsky, A. V., Viskup, A. P., Bashmakov, I. A. and Yaremchenko, A. A., Ceramic microstructure and oxygen permeability of $SrCo(Fe,M)O_{3-\delta}$ (M = Cu or Cr) perovskite membranes. *J. Electrochem. Soc.*, 1998, **145**, 1363–1373.
12. Baker, R. T., Gharbage, B. and Marques, F. M. B., Ionic and electronic conduction in Fe and Cr doped $(La,Sr)GaO_{3-\delta}$. *J. Electrochem. Soc.*, 1997, **144**, 3130–3135.
13. Kharton, V. V., Viskup, A. P., Naumovich, E. N. and Lapchuk, N. M., Mixed electronic and ionic conductivity of $LaCo(M)O_{3-\delta}$ (M = Ga, Cr, Fe or Ni): I. Oxygen transport in perovskites $LaCoO_3$–$LaGaO_3$. *Solid State Ionics*, 1997, **104**, 67–78.
14. Marques, R. M. C., Marques, F. M. B. and Frade, J. R., Characterization of mixed conductors by dc techniques. Part II: Experimental results. *Solid State Ionics*, 1994, **73**, 27–34.
15. Yaremchenko, A. A., Kharton, V. V., Viskup, A. P., Naumovich, E. N., Lapchuk, N. M. and Tikhonovich, V. N., Oxygen ionic and electronic transport in $LaGa_{1-x}Ni_xO_{3-\delta}$ perovskites. *J. Solid State Chem.*, 1999, **142**, 325–335.
16. Slater, P. R., Irvine, J. T. S., Ishihara, T. and Takita, Y., High-temperature powder neutron diffraction study of the oxide ion conductor $La_{0.9}Sr_{0.1}Ga_{0.8}Mg_{0.2}O_{2.85}$. *J. Solid State Chem.*, 1998, **139**, 135–143.
17. Maffei, N. and Kuriakose, A. K., Performance of planar single cell lanthanum gallate based solid oxide fould cells. *J. Power Sources*, 1998, **75**, 162–166.
18. Maric, R., Ohara, S., Fukui, T., Yoshida, H., Nishimura, M., Inagaki, T. and Miura, K., Solid oxide fuel cells with doped lanthanum gallate electrolyte and $LaSrCoO_3$ cathode, and Ni-samaria-doped ceria cermet anode. *J. Electrochem. Soc.*, 1999, **146**, 2006–2010.
19. Kharton, V. V., Yaremchenko, A. A., Patrakeev, M. V., Naumovich, E. N. and Marques, F. M. B., Thermal and chemical induced expansion of $La_{0.3}Sr_{0.7}(Fe,Ga)O_{3-\delta}$ ceramics. *J. Eur. Ceram. Soc.*, 2003, **23**, 1417–1426.
20. Kharton, V. V., Kovalevsky, A. V., Viskup, A. P., Jurado, J. R., Figueiredo, F. M., Naumovich, E. N. and Frade, J. R., Transport properties and thermal expansion of $Sr_{0.97}Ti_{1-x}Fe_xO_{3-\delta}$ ($x = 0.2$–0.8). *J. Solid State Chem.*, 2001, **156**, 437–444.
21. Stevenson, J. W., Armstrong, T. R., Carneim, R. D., Pederson, L. R. and Weber, W. J., Electrochemical properties of mixed conducting perovskites $La_{1-x}M_xCo_{1-y}Fe_yO_{3-\delta}$ (M = Sr, Ba, Ca). *J. Electrochem. Soc.*, 1996, **143**, 2722–2729.
22. Shaula, A. L., Yaremchenko, A. A., Kharton, V. V., Logvinovich, D. I., Naumovich, E. N., Kovalevsky, A. V., Frade, J. R. and Marques, F. M. B., Oxygen permeability of $LaGaO_3$-based ceramic membranes. *J. Membr. Sci.*, 2003, **221**, 69–77.
23. Shaula, A. L., Viskup, A. P., Kharton, V. V., Logvinovich, D. I., Naumovich, E. N., Frade, J. R. and Marques, F. M. B., Oxygen permeability of $LaGa_{0.65}Ni_{0.20}Mg_{0.15}O_{3-\delta}$ ceramics: effect of synthesis method. *Mater. Res. Bull.*, 2003, **38**, 353–362.